RSC Advances

PAPER

View Article Online
View Journal | View Issue

Cite this: *RSC Adv.*, 2020, **10**, 4529

Exploring the inhibitory mechanism of piceatannol on α-glucosidase relevant to diabetes mellitus†

Lili Jiang,[a] Zhen Wang,[a] Xiaoyu Wang,[a] Shujuan Wang,[a] Jun Cao*[b] and Yong Liu *[a]

Received 1st November 2019
Accepted 8th January 2020

DOI: 10.1039/c9ra09028b

rsc.li/rsc-advances

Due to their association with type 2 diabetes mellitus treatment, α-glucosidase inhibitors have attracted increasing attention of researchers. In this study, we systemically investigated the kinetics and inhibition mechanism of piceatannol on α-glucosidase. Enzyme kinetics analyses showed that piceatannol exhibited strong inhibition on α-glucosidase in a non-competitive manner. Spectroscopy analyses indicated that piceatannol could bind with α-glucosidase to form complexes *via* high affinity. Further, computational molecular dynamics and molecular docking studies validated that the binding of piceatannol was outside the catalytic site of α-glucosidase, which would induce conformational changes of α-glucosidase and block the entrance of substrate, causing declines in α-glucosidase activities. Our results provide useful information not only for the inhibition mechanism of piceatannol against α-glucosidase but also for a novel target site for developing novel α-glucosidase inhibitors as potential therapeutic agents in the treatment of type 2 diabetes mellitus.

1. Introduction

Diabetes mellitus (DM) is a group of chronic metabolic diseases affecting millions of people worldwide. As estimated by the World Health Organization (WHO), there will be 642 million people that suffer from DM by 2040,[1] with type 2 diabetes mellitus (T2DM), accounting for up to 90% of these affected patients.[2] Persistent hyperglycemia in diabetes can cause serious complications such as blindness, kidney disease, neuropathy, and cardiovascular disease.[3,4] The goal of the treatment of diabetes mellitus involves lowering blood glucose through blocking carbohydrate digestion and absorption.[5] α-Glucosidase, which is involved in the cleavage of glucose from disaccharides and oligosaccharides, plays an important role in carbohydrate digestion.[6,7] Therefore, the inhibitors of this enzyme can reduce postprandial hyperglycemia, and have been recognized as new anti-diabetic drug candidates. Several oral drugs, such as acarbose, voglibose, and miglitol,[8–10] have been used to inhibit the α-glucosidase activity in patients with T2DM. However, these drugs often showed several side effects such as meteorism, abdominal distention, and liver disorders.[11] Therefore, much effort has been undertaken to find natural and safer α-glucosidase inhibitors without possibly harmful side effects.

Natural products of great structural diversity are considered as a good source for screening α-glucosidase inhibitors.[12] In recent years, phenolic compounds have received much attention, and several phenolic compounds have shown significant inhibitory effects against α-glucosidase. Li *et al.* reported that gallotannin had a strong α-glucosidase inhibitory effect (IC_{50} = 1.31 μM) in a parabolic mixed-type manner.[13] The polyphenol extract of *Geranium collinum* root was found to show inhibitory activity on α-glucosidase *in vitro*.[14] Moreover, some other phenolic compounds, such as green tea polyphenols,[15] water extract of black tea,[16] phloretin in apple[2] and apigenin in celery,[17] have revealed significant inhibition of α-glucosidase activity and alleviated the symptoms of type 2 diabetes.

Piceatannol is a polyphenolic phytochemical, belonging to a natural analog of resveratrol.[18] Piceatannol is abundant in various fruits, such as *Vaccinium* berries (138–422 ng g^{-1}),[19] red grapes (374 ng g^{-1}),[20] and passion fruit seeds (4.8 mg g^{-1}).[21] Piceatannol has a wide spectrum of biological activity, such as vasorelaxant effects, antibacterial activity, antioxidant and pro-oxidant activities.[20,22] Piceatannol has also been suggested to be an inhibitor of α-glucosidase.[23] However, the effects of piceatannol on α-glucosidase activity have not been fully characterized. Moreover, few studies have reported the specific ligand-binding mechanisms of piceatannol to α-glucosidase molecule.[24] Understanding the effect of piceatannol on α-glucosidase activity and its mechanism is important to ensure its safe administration and develop new functional food.

The aim of this study was to investigate the inhibition effect and its possible mechanism of piceatannol on α-glucosidase by using a combination of UV-vis and fluorescence spectral analysis, enzyme kinetic analysis as well as molecular docking

[a]*School of Life and Pharmaceutical Sciences, Dalian University of Technology, 2 Dagong Road, Liaodongwan New District, Panjin 124221, China. E-mail: yliu@dlut.edu.cn*

[b]*Department of Occupational and Environmental Health, Dalian Medical University, No. 9 W. Lvshun South Road, Dalian 116044, China. E-mail: caojunly@163.com*

† Electronic supplementary information (ESI) available. See DOI: 10.1039/c9ra09028b

methods. This study provides some significant clues to improving the applications of piceatannol in functional food for the prevention and treatment of type 2 diabetes and also suggests a novel target site for developing novel α-glucosidase inhibitors.

2. Materials and methods

2.1 Materials

α-Glucosidase from *Saccharomyces cerevisiae* (EC 3.2.1.20, 50.3 U mg^{-1}), 4-nitrophenyl-β-D-glucopyranosiduronic acid (*p*NPG), and acarbose were obtained from Sigma-Aldrich (St, Louis, USA). *p*-Nitrophenol (*p*NP) was purchased from Aladdin Biotechnology (Shanghai, China). Piceatannol was purchased from Selleck Chemicals (USA). All other chemicals were of analytical reagent grade, and their aqueous solutions were prepared with freshly ultrapure water.

2.2 α-Glucosidase inhibition assay

The α-glucosidase inhibitory activity assay was performed according to the methods described by previous reports with minor modifications.[25,26] The enzyme was incubated with varying concentrations of piceatannol in a 100 mM phosphate buffer (pH 6.8) at 37 °C. The substrate reaction mixture contained 0.6 mM *p*NPG substrate in a 100 mM phosphate buffer (pH 6.8) with and without piceatannol at various concentrations. The enzyme activity assay was conducted following incubation at 37 °C for 7 min.

The percentage inhibition of α-glucosidase activity was calculated using the following equation:

$$\text{Inhibition } (\%) = \frac{A_i}{A_0} \times 100\%$$

where A_0 is the activity of the enzyme without piceatannol and A_i is the activity of the enzyme with piceatannol at different concentrations.

2.3 Inhibitory kinetic analysis

Inhibition constant (K_i) values were determined using various concentrations of *p*NPG in the presence or absence of piceatannol. K_i values were calculated by nonlinear regression using the equations for competitive inhibition (eqn (1)), non-competitive inhibition (eqn (2)), or mixed inhibition (eqn (3)):

$$\frac{1}{v} = \frac{K_m}{V_{max}}\left(1 + \frac{[I]}{K_i}\right)\frac{1}{[S]} + \frac{1}{V_{max}} \quad (1)$$

$$\frac{1}{v} = \frac{K_m}{V_{max}}\left(1 + \frac{[I]}{K_i}\right)\frac{1}{[S]} + \frac{1}{V_{max}}\left(1 + \frac{[I]}{K_i}\right) \quad (2)$$

$$\frac{1}{v} = \frac{K_m}{V_{max}}\left(1 + \frac{[I]}{K_i}\right)\frac{1}{[S]} + \frac{1}{V_{max}}\left(1 + \frac{[I]}{\alpha K_i}\right) \quad (3)$$

A secondary plot can be acquired from

$$\text{slope} = \frac{K_m}{V_{max}} + \frac{K_m[I]}{V_{max}K_i}$$

where v is the enzyme reaction rate in the absence and presence of inhibitors. The Michaelis–Menten constant and inhibition constant are expressed as K_m and K_i, respectively. α is the apparent coefficient. [I] and [S] are the concentrations of inhibitor and substrate, respectively. The linearly fitted secondary plots of slope *vs.* [I] suggest the existence of one or a class of inhibition sites. The kinetic process and inactivation rate constants were obtained using time-course measurements.

2.4 Fluorescence spectra measurements

A 2.0 mL substrate reaction mixture containing 6.96×10^{-2} μM α-glucosidase was added to a 1.0 cm quartz cuvette, and then the solution was titrated by successive additions of piceatannol (the final concentrations of piceatannol were varied from 0 to 1.46 μM). These solutions were allowed to stand for 5 min to equilibrate, and then the fluorescence spectra at three temperatures (209, 304 and 310 K) were measured on a Hitachi spectrofluorometer (Model F-7000, Hitachi, Japan) in the wavelength range of 290–500 nm by exciting at 280 nm. Both excitation and emission slit widths were set at 2.5 nm. The appropriate blanks, corresponding to the sodium phosphate buffer (pH 6.8) and the piceatannol, were deducted to correct the fluorescence background.

To differentiate the dynamic and static quenching, the quenching effect of piceatannol was further investigated by the Stern–Volmer equation:[27]

$$\frac{F_0}{F} = 1 + K_{SV}[Q] = 1 + K_q\tau_0[Q]$$

where F_0 and F are the fluorescence intensities of α-glucosidase in the absence and presence of piceatannol, respectively. K_q is the quenching rate constant of the biomolecule ($K_q = K_{SV}/\tau_0$). K_{SV} is the Stern–Volmer dynamic quenching constant, which is determined by linear regression of a plot of F_0/F against [Q]. τ_0 is the average lifetime of the fluorophore without piceatannol, which is equal to 10^{-8} s.

The number of binding sites of piceatannol on α-glucosidase was determined by the following the double-logarithm equation:[28]

$$\log\frac{F_0 - F}{F} = n\log K_a - n\log\frac{1}{[Q_t] - \frac{(F_0 - F)[P_t]}{F_0}}$$

where $[Q_t]$ and $[P_t]$ denote the total concentration of the piceatannol and α-glucosidase, respectively. K_a represents the binding constant for the accessible fluorophores, n is the number of the binding sites per α-glucosidase molecule.

Thermodynamic parameters were calculated by the van't Hoff equation as follows:

$$\log K_a = -\frac{\Delta H}{2.303RT} + \frac{\Delta S}{2.303R}$$

where R is the gas constant (8.314 J mol^{-1} K^{-1}), and T represents the experimental temperature at 298, 304 and 310 K. The values of ΔH and ΔS were calculated from the slope and intercept of the linear plot of $\log K_a$ *versus* $1/T$, and the free energy change (ΔG) was estimated from the following relationship:

$$\Delta G = \Delta H - T\Delta S$$

Synchronous fluorescence spectra were measured by maintaining the interval of the excitation wavelength and emission wavelength constant ($\Delta\lambda = \lambda_{em} - \lambda_{ex}$) at 15 nm and 60 nm, respectively.[29]

Because of re-absorption, the fluorescence data were corrected for the absorption of the excitation and emitted light to eliminate the re-absorption and inner filter effects caused by UV absorption, according to the following relationship:[30,31]

$$F_c = F_m e^{(A_{ex}+A_{em})/2}$$

where F_c and F_m represent the corrected and measured fluorescence, respectively. A_{ex} and A_{em} are the absorbance of the mixed solution of piceatannol and α-glucosidase at the excitation and emission wavelengths, respectively.

2.5 Homology modeling and molecular docking studies

A three-dimensional (3D) structure of α-glucosidase was built on the Swiss Modeling server (https://swissmodel.expasy.org/interactive) using homology modeling based on the X-ray structure of the isozyme (PDB ID: 5NN3), which has a high sequence identity and residues similarity to the target protein sequence (GenBank: ABI53718.1).[32] The final model was optimized using PROCHECK (http://servicesn.mbi.ucla.edu/SAVES/). ESI Fig. 1 and 2† provide a summary of the homology modelling parameters and the Ramachandran plot analysis of the homology model, respectively.

Based on a previous computational study,[33] the molecular docking was performed by means of the Autodock version 4.2 program. The homology model was used as the receptor model, the Gasteiger charges and polar hydrogen bonds were added to the macromolecule file. The 3D structures of small molecules were prepared using Chem3D Ultra 8.0. Then, the docking simulations were carried out with the Lamarckian genetic algorithm for 100 docking runs and were extended over the whole receptor protein to find visible combination models. In the process of docking, the remaining parameters were set as default. The lowest energy conformation of the more populated cluster was considered as the most reliable solution.

2.6 Statistical analysis

Data were expressed as means ± standard deviation ($n = 3$). Data were analyzed by nonlinear regression using the Graphpad Prism 5 software, $p < 0.05$ was considered statistically significant.

3. Results

3.1 Inhibition effect of piceatannol on α-glucosidase activity

The α-glucosidase inhibitory activity of piceatannol is presented in Fig. 1. The results revealed that piceatannol significantly inhibited α-glucosidase activity in a dose-dependent manner (Fig. 1). The half-maximal inhibitory concentration (IC_{50}) of piceatannol and acarbose, a known inhibitor, against α-glucosidase were calculated as 4.39 ± 0.74 μM and 647.70 ± 1.09 μM, respectively. Piceatannol exerted a more potent inhibitory effect on α-glucosidase activity than that of acarbose.

3.2 Kinetics of inhibition

The kinetic experiments were performed to further characterize the inhibition of α-glucosidase activity by piceatannol. Piceatannol strongly inhibited the formation of *p*NP by α-glucosidase. Plots of the reaction velocity (υ) *versus* [α-glucosidase] at various concentrations of piceatannol were shown in Fig. 2A. The results showed that all straight lines passed through the origin, whose slopes were dropped with the increase in piceatannol concentration, indicating that the inhibition of α-glucosidase by piceatannol was reversible.

Changes in V_{max} values were observed on the Lineweaver–Burk plots (Fig. 2B). Obviously, the value of V_{max} decreased, whereas $-1/K_m$ was constant with the increasing concentrations of inhibitors, and all the lines crossed the negative direction of the horizontal axis. Together the data suggested that the inhibition followed a typical non-competitive mechanism. The value of the inhibition constant (K_i) was calculated to be 5.38 ± 0.24 μM. Furthermore, the secondary plots of the slope and *Y*-intercept *versus* [piceatannol] were linear, indicating that one or a class of inhibition sites existed in α-glucosidase with respect to the piceatannol (Fig. 2C and D).

3.3 Quenching of α-glucosidase fluorescence by piceatannol

3.3.1 Mechanism of fluorescence quenching. To confirm the interaction between piceatannol and α-glucosidase, the intrinsic fluorescence spectra of α-glucosidase in the presence of piceatannol were examined by the fluorescence quenching experiments. As shown in Fig. 3A–C, with the addition of piceatannol, the fluorescence intensity of α-glucosidase was gradually reduced, indicating that piceatannol interacted with α-glucosidase.

As observed in Fig. 3D, K_{SV} values increased with increasing temperature, suggesting that the quenching of α-glucosidase by piceatannol was a dynamic process. However, the calculated values of K_q (5.02×10^{13}, 7.01×10^{13}, 16.04×10^{13} L mol^{-1} s^{-1} at 298, 304 and 310 K, respectively) were obviously greater than 2×10^{10} L mol^{-1} s^{-1}, indicating that the fluorescence quenching process was dominated by a static procedure resulting from the piceatannol–α-glucosidase complex formation. These results indicated that the quenching of α-glucosidase by piceatannol was a combination of dynamic and static processes.

As shown in Table 1, the values of n were approximately equal to 1, suggesting that there was one binding site on α-glucosidase for piceatannol, and the result was consistent with that mentioned above. Moreover, in accordance with the alteration in K_{SV}, K_a increased with temperature from 298 K to 310 K. The K_a values were in the order of 10^5 to 10^6 L mol^{-1}, suggesting that a high affinity existed between piceatannol and α-glucosidase.

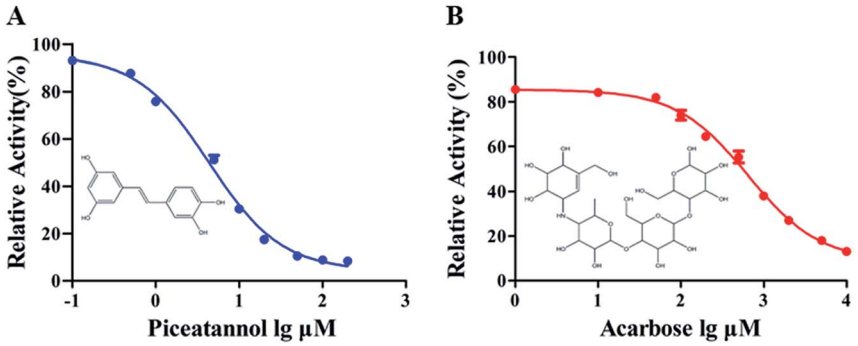

Fig. 1 The effects of piceatannol and acarbose on the activity of α-glucosidase.

3.3.2 Thermodynamic parameters and the nature of the binding forces. As revealed in Table 1, the binding process was spontaneous since the value of ΔG was below zero. Furthermore, the positive values of ΔH and ΔS indicated that the formation of the piceatannol–α-glucosidase complex was an endothermically and entropically increased process, and the values were frequently regarded as typical evidence for hydrophobic interactions. Therefore, piceatannol–α-glucosidase complexation was mainly driven by hydrophobic forces.

3.3.3 Synchronous fluorescence. Synchronous fluorescence spectra can reflect the micro-environmental changes in tyrosine (Tyr) and tryptophan (Trp) residues when the $\Delta\lambda$ between the excitation and emission wavelengths were stabilized at 15 nm and 60 nm, respectively. The maximum fluorescence emission peak (λ_{max}) of Tyr displayed no discernable shift, indicating that

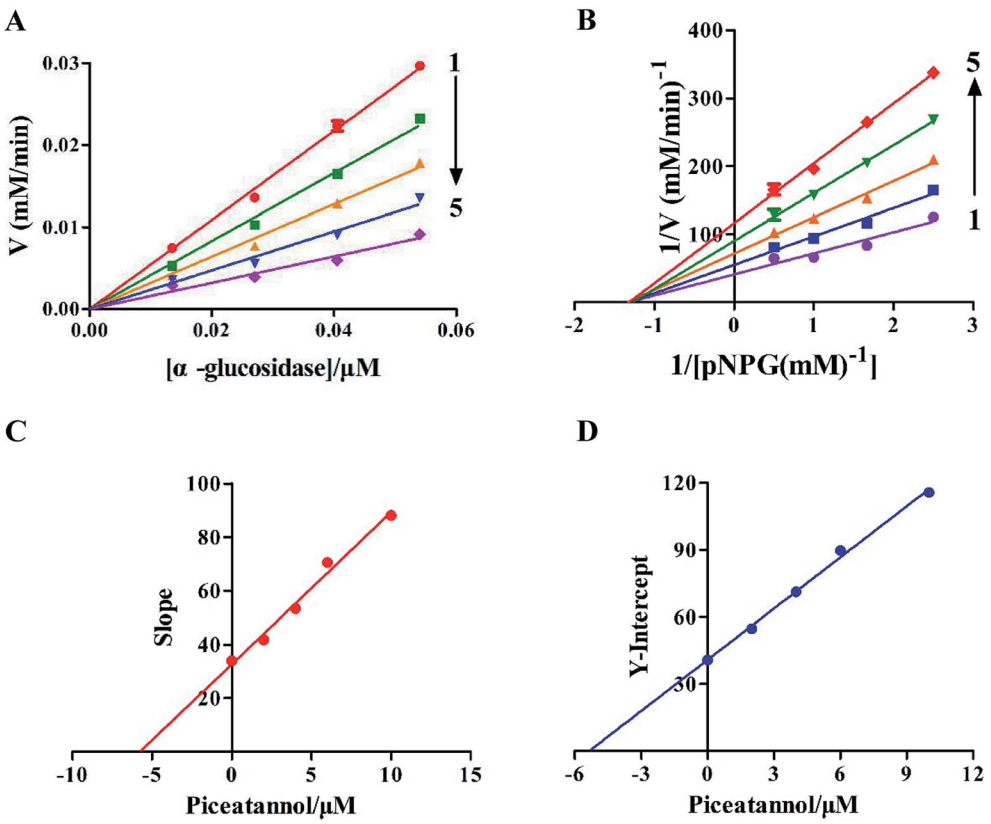

Fig. 2 Inhibition kinetics of piceatannol on α-glucosidase: (A) plots of v *versus* [α-glucosidase]. The piceatannol concentrations were 0, 2, 4, 6 and 10 μM for curves 1 → 5, respectively. The vertical v indicated the reaction velocity at piceatannol concentrations of 0, 2, 4, 6 and 10 μM in 100 μL. [α-glucosidase] indicates the α-glucosidase final concentration (1.35×10^{-2}, 2.70×10^{-2}, 4.05×10^{-2}, and 5.40×10^{-2} μM). (B) Lineweaver–Burk plots of the reversible inhibition of piceatannol on α-glucosidase. The piceatannol concentrations were 0, 2, 4, 6 and 10 μM for curves 1 → 5. c(α-Glucosidase) = 6.96×10^{-2} μM. (C) The secondary plot of slope *versus* [piceatannol]. The *Y*-axis is the slope of the primary plots (Lineweaver–Burk plots). (D) The secondary plot of the *Y*-intercept *versus* [piceatannol]. The *Y*-axis is the *Y*-intercept of the primary plots (Lineweaver–Burk plots).

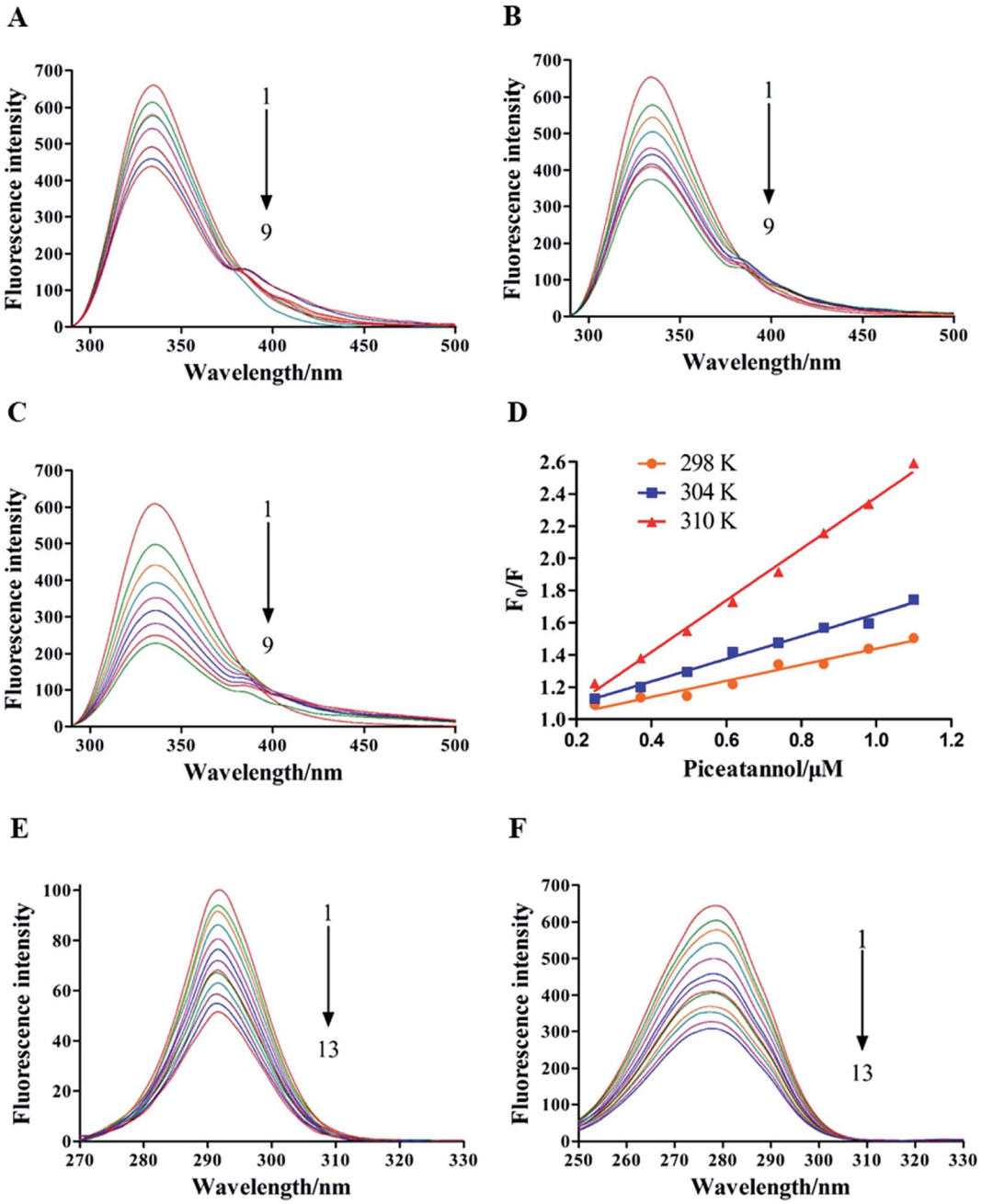

Fig. 3 Fluorescence spectra of α-glucosidase in the absence and presence of piceatannol at different concentrations: (A) $T = 298$ K, (B) $T = 304$ K, (C) $T = 310$ K. c(α-Glucosidase) $= 6.96 \times 10^{-2}$ μM, and c(piceatannol) $= 0$, 0.25, 0.37, 0.50, 0.62, 0.74, 0.86, 0.98 and 1.10 μM for curve 1 → 9, respectively. (D) Stern–Volmer plots for the fluorescence quenching of α-glucosidase by piceatannol at different temperatures. Synchronous fluorescence spectra of α-glucosidase in the absence and presence of piceatannol. (E) $\Delta\lambda = 15$ nm, (F) $\Delta\lambda = 60$ nm (pH = 6.4, $T = 304$ K). c(α-Glucosidase) $= 6.96 \times 10^{-2}$ μM, and c(piceatannol) $= 0$, 0.13, 0.25, 0.37, 0.50, 0.62, 0.74, 0.86, 0.98, 1.10, 1.2, 1.3 and 1.46 μM for curves 1 → 13, respectively.

Table 1 Quenching constants K_{SV}, binding constants K_a and relative thermodynamic parameters of the piceatannol and α-glucosidase interactions at different temperatures. R^a is the correlation coefficient for the K_{SV} values. R^b is the correlation coefficient for the K_a values

T (K)	K_{SV} ($\times 10^5$ L mol^{-1})	R^a	K_a ($\times 10^5$ L mol^{-1})	n	R^b	ΔH° (kJ mol^{-1})	ΔG° (kJ mol^{-1})	ΔS° (J mol^{-1} K^{-1})
298	5.02 ± 0.039	0.98	4.93	1.17 ± 0.057	0.99	64.55 ± 9.67	−32.39 ± 9.64	325.31 ± 31.80
304	7.01 ± 0.032	0.99	7.24	1.16 ± 0.045	1.00		−34.34 ± 9.64	
310	16.04 ± 0.049	0.99	13.54	1.32 ± 0.017	1.00		−36.30 ± 9.64	

piceatannol had no influence on the microenvironment of Tyr residues of α-glucosidase (Fig. 3E). However, an apparent blue shift (from 278.6 nm to 277.6 nm) of the λ_{max} was observed on Trp, suggesting that the interactions between piceatannol and α-glucosidase obviously changed the microenvironment of Trp and increased its hydrophobicity (Fig. 3F).

3.4 The binding site of piceatannol on α-glucosidase

The evaluation results of PROCHECK showed that 91.3%, 8.5% and 0.1% of the residues were located within the most favorable, additionally allowed and generously allowed regions of the Ramachandran plot, respectively. The results indicated that the homology model was suitable for the following molecular docking study.

To expound the binding mode of piceatannol on α-glucosidase, molecular docking was carried out. The results showed that acarbose, a known competitive inhibitor, was bound to the active cavity of α-glucosidase and inhibited the catalytic action of α-glucosidase through hydrogen bonds and van der Waals forces (Fig. 4). As shown in Fig. 5, piceatannol was mainly surrounded by amino acid residues Lys 96, Ile 98, Gln 124, Gly 116, Leu 117, Ala 113, Gly 123, Trp 126, Ala 93 and Ala 97 of α-glucosidase, and hydrogen bonds were formed between hydroxyl groups and amino acid residues Lys 96, Ile 98, Gln 124. Furthermore, hydrophobic interactions were formed between piceatannol and the residues Gly 116, Leu 117, Ala 113, Gly 123, Trp 126, Ala 93 and Ala 97 of α-glucosidase, indicating that the hydrophobic interactions were another force in the binding of piceatannol with α-glucosidase. These results indicate that all potential binding sites of piceatannol with α-glucosidase were away from the active cavities of the enzyme, which is also in agreement with the experimental results.

4. Discussion

Our data offer *in vitro* evidence that piceatannol, a hydroxylated analog of resveratrol, is a potent non-competitive inhibitor of α-glucosidase. Resveratrol with antidiabetic effect has been reported to be a good inhibitor of α-glucosidase.[2,34] Interestingly, the observed inhibitory effect against α-glucosidase by piceatannol in the current study is much more potent than that demonstrated by resveratrol,[35] which may be structure related. Compared with resveratrol, piceatannol has an additional hydroxy group at the 8′-position. A previous study reported that the inhibition activity on α-glucosidase was increased while adding hydroxyl groups to the B ring of flavones.[36] Moreover, a recent study from Liu *et al.*[37] also indicated that the positions

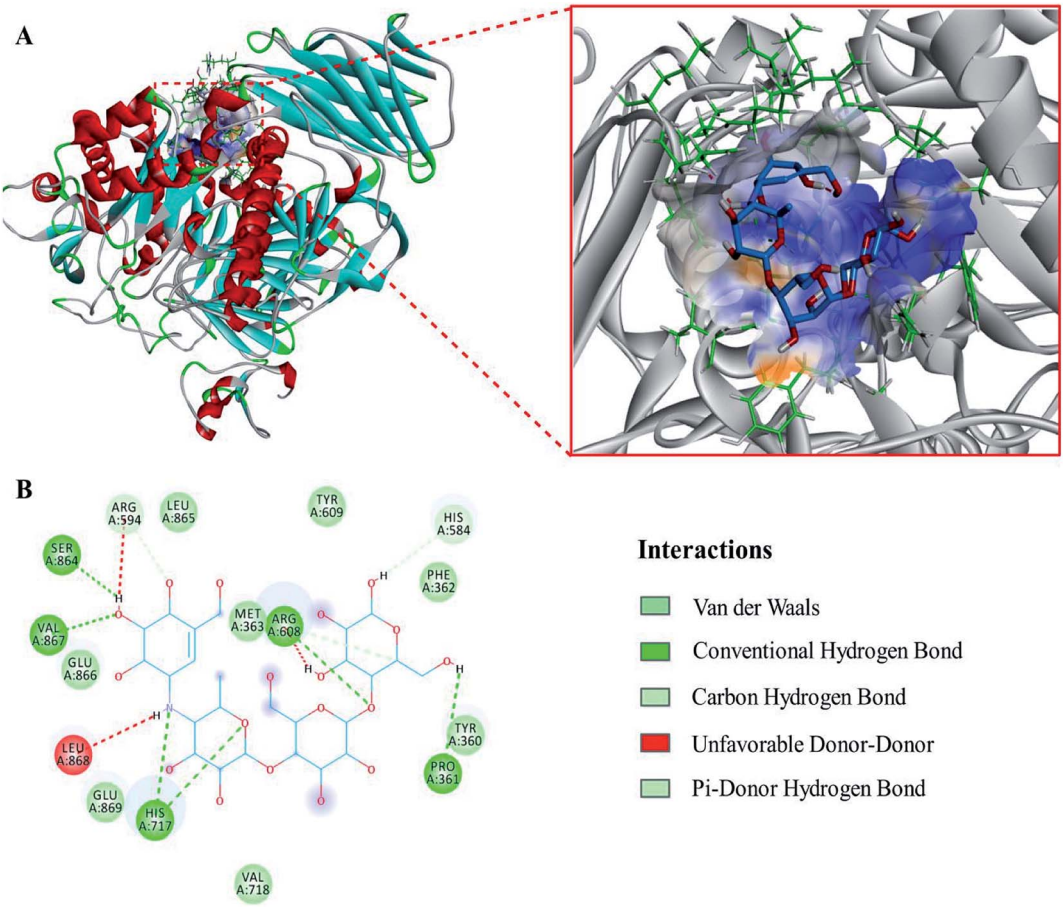

Fig. 4 (A) The corresponding surface structure of α-glucosidase interacting with acarbose (ligands are represented as sticks and balls, protein as ribbons). (B) 2D interaction diagram of α-glucosidase with acarbose (H-bonds are represented as green dotted lines).

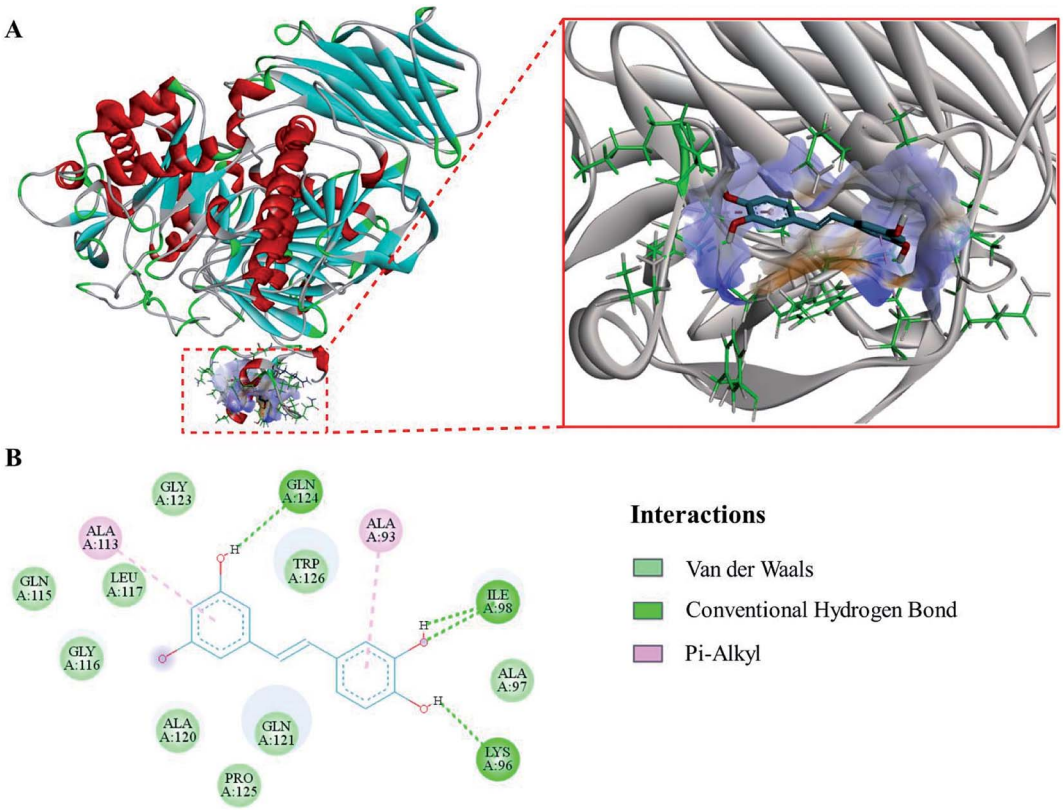

Fig. 5 (A) The corresponding surface structure of α-glucosidase interacting with piceatannol (ligands are represented as sticks and balls, protein as ribbons). (B) 2D interaction diagram of α-glucosidase with piceatannol (H-bonds are represented as green dotted lines).

of the hydroxyl groups of the polyphenols had an important influence on their interactions with enzymes and the enzyme activities. It is likely that the additional hydroxyl group at this position is conducive to the distribution of the electron cloud, which causes the hydroxyl group to form hydrogen bonds with α-glucosidase.

From the fluorescence spectra, an apparent blue shift in λ_{max} was observed on the Trp, suggesting that the interactions between piceatannol and α-glucosidase resulted in significant variations in Trp residues or conformational changes.[38] Moreover, the formation of the piceatannol–α-glucosidase complex was an endothermically and entropically increased process, which is frequently regarded as typical evidence for hydrophobic interactions.[39] Therefore, we suggest that piceatannol–α-glucosidase complexation could be driven by hydrophobic forces. These assumptions were further verified in our docking study.

According to the quenching theory, the quenching mechanisms of piceatannol included both dynamic and static processes. These phenomena are different from other potent α-glucosidase inhibitors, for example, quercetin, isoquercetin[40] and butylisobutyl-phthalate (BIP)[41] all of which formed a stable complex. Furthermore, there was a high affinity between piceatannol and α-glucosidase. Therefore, we speculate that the potent inhibitory effect of piceatannol might due to its combination with α-glucosidase and could consequently induce conformational changes in the enzyme. This binding mechanism of piceatannol to α-glucosidase was different from that of other proteins, such as bovine serum albumin (BSA).[42]

In our docking study, we found that the binding site of piceatannol was at a hydrophobic pocket outside of the catalytic site of α-glucosidase, and the binding could block the entrance of other substrates. This hydrophobic pocket, which contained Lys 96, Ile 98, Gln 124, was different from the binding pocket of acarbose, a known competitive inhibitor.[43] These results suggest that piceatannol and acarbose could bind to α-glucosidase at different sites. The docking simulation in our study provides a novel target site outside the catalytic site for developing and designing novel α-glucosidase inhibitors.

5. Conclusions

The present study has systemically investigated the inhibitory effects of piceatannol on α-glucosidase and has provided new insights into the inhibitory and interaction mechanisms of piceatannol on α-glucosidase. This study demonstrates that piceatannol is a vital and potent α-glucosidase inhibitor. Further studies suggest that the interaction between piceatannol and α-glucosidase is a combination of dynamic and static processes, and is mainly driven by hydrophobic interactions. Moreover, the non-competitive inhibition of piceatannol against α-glucosidase may be due to the binding of piceatannol outside the active site of α-glucosidase. These results provide useful information not only for the inhibition mechanism of

piceatannol against α-glucosidase, but also provide a basis for further application of piceatannol in novel functional foods or antidiabetic drugs.

Abbreviations

DM	Diabetes mellitus
WHO	World health organization
T2DM	Type 2 diabetes mellitus
*p*NPG	4-Nitrophenyl-β-D-glucopyranosiduronic acid
*p*NP	*p*-Nitrophenol
Tyr	Tyrosine
Trp	Tryptophan
BIP	Butylisobutyl-phthalate

Authors' contributions

Study conception and design: Yong Liu, Jun Cao. Performing of the research: Lili Jiang, Zhen Wang. Analysis and interpretation of data: Zhen Wang, Xiaoyu Wang, Shujuan Wang. Drafting of manuscript: Lili Jiang, Zhen Wang. Critical revision: Yong Liu, Jun Cao.

Conflicts of interest

The authors declare that there is no conflict of interests regarding the publication of this article.

Acknowledgements

This study was financially supported by the National Key Research and Development Program of China (2017YFC1702006), the Dalian Science and Technology Innovation Foundation (2018J13SN114).

References

1 World Health Organization, avaiable from: https://www.who.int/diabetes/global-report, 2016, accessed February 11, 2019.
2 A. J. Zhang, A. M. Rimando, C. S. Mizuno and S. T. Mathews, *J. Nutr. Biochem.*, 2017, **47**, 86–93.
3 D. M. Nathan, *N. Engl. J. Med.*, 1993, **328**, 1676–1685.
4 W. Duckworth, C. Abraira, T. Moritz, D. Reda, N. Emanuele, P. D. Reaven, F. J. Zieve, J. Marks, S. N. Davis, R. Hayward, S. R. Warren, S. Goldman, M. McCarren, M. E. Vitek, W. G. Henderson and G. D. Huang, *N. Engl. J. Med.*, 2009, **360**, 129–139.
5 G. S. Chadha and M. E. Morris, *AAPS J.*, 2015, **17**, 1464–1474.
6 J. Poongunran, H. K. Perera, L. Jayasinghe, I. T. Fernando, R. Sivakanesan, H. Araya and Y. Fujimoto, *Pharm. Biol.*, 2017, **55**, 206–211.
7 S. Kumar, S. Narwal, V. Kumar and O. Prakash, *Pharmacogn. Rev.*, 2011, **5**, 19–29.
8 R. K. Singla, R. Singh and A. K. Dubey, *Curr. Top. Med. Chem.*, 2016, **16**, 2625–2633.
9 K. Kaku, *Expert Opin. Pharmacother.*, 2014, **15**, 1181–1190.
10 L. J. Scott and C. M. Spencer, *Drugs*, 2000, **59**, 521–549.
11 K. R. Rengasamy, M. A. Aderogba, S. O. Amoo, W. A. Stirk and J. Van Staden, *Food Chem.*, 2013, **141**, 1412–1415.
12 X. Peng, G. Zhang, Y. Liao and D. Gong, *Food Chem.*, 2016, **190**, 207–215.
13 L. M. Yue, J. Lee, L. Zheng, Y. D. Park, Z. M. Ye and J. M. Yang, *Int. J. Biol. Macromol.*, 2017, **103**, 829–838.
14 S. Numonov, S. Edirs, K. Bobakulov, M. N. Qureshi, K. Bozorov, F. Sharopov, W. N. Setzer, H. Zhao, M. Habasi, M. Sharofova and H. A. Aisa, *Molecules*, 2017, **22**, 983.
15 X. Yang and F. Kong, *J. Sci. Food Agric.*, 2016, **96**, 777–782.
16 D. P. Tong, K. X. Zhu, X. N. Guo, W. Peng and H. M. Zhou, *Int. J. Biol. Macromol.*, 2018, **107**, 129–136.
17 L. Zeng, G. Zhang, S. Lin and D. Gong, *J. Agric. Food Chem.*, 2016, **64**, 6939–6949.
18 H. Uchida-Maruki, H. Inagaki, R. Ito, I. Kurita, M. Sai and T. Ito, *Biol. Pharm. Bull.*, 2015, **38**, 629–633.
19 A. M. Rimando, W. Kalt, J. B. Magee, J. Dewey and J. R. Ballington, *J. Agric. Food Chem.*, 2004, **52**, 4713–4719.
20 H. Piotrowska, M. Kucinska and M. Murias, *Mutat. Res.*, 2012, **750**, 60–82.
21 J. Kershaw and K. H. Kim, A Review, *J. Med. Food*, 2017, **20**, 427–438.
22 S. Sano, K. Sugiyama, T. Ito, Y. Katano and A. Ishihata, *J. Agric. Food Chem.*, 2011, **59**, 6209–6213.
23 M. Minakawa, Y. Miura and K. Yagasaki, *Biochem. Biophys. Res. Commun.*, 2012, **422**, 469–475.
24 H. He and Y. H. Lu, *J. Agric. Food Chem.*, 2013, **61**, 8110–8119.
25 J. Q. Zhao, Y. M. Wang, Y. L. Yang, Y. Zeng, Q. L. Wang, Y. Shao, L. J. Mei, Y. P. Shi and Y. D. Tao, *Food Chem.*, 2017, **227**, 93–101.
26 E. Apostolidis, Y. I. Kwon and K. Shetty, *Innovative Food Sci. Emerging Technol.*, 2007, **8**, 46–54.
27 A. Bhogale, N. Patel, P. Sarpotdar, J. Mariam, P. M. Dongre, A. Miotello and D. C. Kothari, *Colloids Surf., B*, 2013, **102**, 257–264.
28 S. R. Feroz, S. B. Mohamad, Z. S. D. Bakri, S. N. A. Malek and S. Tayyab, *PLoS One*, 2013, **8**, e76067.
29 Y. Wang, G. Zhang, J. Pan and D. Gong, *J. Agric. Food Chem.*, 2015, **63**, 526–534.
30 X. Wu, J. Liu, H. Huang, W. Xue, X. Yao and J. Jin, *Int. J. Biol. Macromol.*, 2011, **49**, 343–350.
31 G. Zhang, N. Zhao and L. Wang, *J. Lumin.*, 2011, **131**, 880–887.
32 G. C. Wang, M. Chen, J. Wang, Y. P. Peng, L. Y. Li, Z. Z. Xie, B. Deng, S. Chen and W. B. Li, Synthesis, biological evaluation and molecular docking studies of chromone hydrazone derivatives as α-glucosidase inhibitors, *Bioorg. Med. Chem. Lett.*, 2017, **27**, 2957–2961.
33 X. Li, Z. R. Lü, W. Wang, X. P. Han, J. M. Yang, Y. D. Park, H. M. Zhou, Q. Sheng and J. Lee, Effect of Ba^{2+} on the activity and structure of α-glucosidase: inhibition kinetics and molecular dynamics simulation, *Process Biochem.*, 2015, **50**, 582–588.

34 A. M. Rimando, R. Nagmani, D. R. Feller and W. Yokoyama, *J. Agric. Food Chem.*, 2005, **53**, 3403–3407.
35 Y. Zhao, M. X. Chen, K. T. Kongstad, A. K. Jager and D. Staerk, *J. Agric. Food Chem.*, 2017, **65**, 4421–4427.
36 J. Xiao, G. Kai, K. Yamamoto and X. Chen, *Crit. Rev. Food Sci. Nutr.*, 2013, **53**, 818–836.
37 M. Liu, T. T. Liu, Y. B. Shi, Y. N. Zhao, H. Yan, B. Sun, Q. P. Wang, Z. P. Wang and J. Han, *Food Funct.*, 2019, **12**, 8182–8194.
38 F. Xiao, M. Gu, Y. Liang, L. Li and Y. Luo, *Spectrochim. Acta, Part A*, 2014, **118**, 1106–1112.
39 P. D. Ross and S. Subramanian, *Biochemistry*, 1981, **20**, 3096–3102.
40 M. Liu, W. Zhang, L. Qiu and X. Lin, *J. Biochem.*, 2011, **149**, 27–33.
41 Y. Q. Li, F. C. Zhou, F. Gao, J. S. Bian and F. Shan, *J. Agric. Food Chem.*, 2009, **57**, 11463–11468.
42 X. Xu, M. S. Zhao, Q. Q. Han, H. J. Wang, H. M. Zhang and Y. Q. Wang, *Spectrochim. Acta, Part A*, 2019, 117706.
43 K. Bharatham, N. Bharatham, K. H. Park and K. W. Lee, *J. Mol. Graphics Modell.*, 2008, **26**, 1202–1212.